Review of the precise orbit determination for Chinese lunar exploration projects

Shanhong Liu[1, 4], Jianguo Yan[1, *], Jianfeng Cao[2], Mao Ye[1, *], Xie Li[2], Fei Li[1], and Jean-Pierre Barriot[1, 3]

[1]State Key Laboratory of Information Engineering in Surveying, Mapping and Remote Sensing, Wuhan University, 430079 Wuhan, China

[2]Beijing Aerospace Flight and Control Center, 100094 Beijing, China

[3]Observatoire géodésique de Tahiti, University of French Polynesia, 98702 Faa'a, BP 6570 Tahiti, French Polynesia

[4]Observatoire de la Côte d'Azur, Geoazur, CNRS UMR7329 Valbonne, France

Corresponding author: Jianguo Yan (jgyan@whu.edu.cn); Mao Ye (mye@whu.edu.cn)

Abstract

China's lunar exploration missions have developed and progressed for more than 13 years. In these missions, Precise Orbit determination (POD) guarantees successful execution of Chang'e missions, and the basis for further scientific investigations using radio science data; for example, recovering the lunar gravity field to explore the inner structure and detect craters to study the evolutionary history of the moon. This paper briefly reviews the Chang'e series mission orbit and tracking measurements. We reprocessed the tracking data and comprehensively summarized the evolution in POD accuracy and the tracking system precision from the Chang'e 1 to Chang'e 4 missions. Our results show that the accuracy of Chang'e 5T1 Doppler measurements reach about 0.35 mm/s and the two-way range measurements 0.2 m, with respect to 1.1 mm/s and 1.6 m for Chang'e 1. The Chang'e 4 relay satellite achieved POD accuracy at the meter level, in contrast to the half-kilometer level accuracy achieved during the Chang'e 1 mission. We can clearly see that the POD performance and precision of the Chang'e spacecraft are continuously improving. This research is a reference for future Chinese Lunar missions, as well as Chinese Mars and asteroid explorations.

Keywords: Moon, precise orbit determination, data analysis

1 Introduction

Lunar exploration continually attracts the interest and excitement of scientists worldwide. In past 60 years, the humans have carried out more than 100 lunar exploration missions with a cheered history. The first spacecraft to reach the Moon was the Soviet Luna 2 spacecraft, which hit the lunar surface on the 13th September 1959. In the same year, Luna 3 completed the first flyby of the Moon (Harvey 2006). After that, US started lunar exploration. Between 1962 and 1965, US lunched Ranger probes to pave the way for the Surveyor series (between 1966 and 1968) of robotic soft landers (Sjogren, et al 1966). The Luna 9 and 10 missions from the Soviet Union and Lunar Orbiter missions from the US were launched in the same period, from 1966 to 1967 (Akim 1967; Lorell & Sjogren 1968). Between 1968 and 1976, the Apollo series from US overlapped with Luna series mission from Soviet Union were successfully executed, and have left an enduring scientific legacy (Wihelms,1993; Crawford, et al., 2014; Heiken, et al., 1991; Crawford, 2012). After the Luna 24 mission, there was almost a twenty-year gap in lunar

exploration. The lunar exploration was active again in the 1990s with the Hiten from Japan, Clementine and Lunar Prospector (LP) from US flying to the Moon (Uesugi et al., 1991; Nozette et al.,1994; Binder 1998).

Entering the 21st century, the pace of lunar exploration has accelerated, driven by the National Aeronautics and Space Administration (NASA, US), European Space Agency (ESA), Japan Aerospace Exploration Agency (JAXA), China National Space Administration (CASA) and Indian Space Research Organization (ISRO), with more than a dozen probes sent to the Moon for scientific exploration. These missions include SMART-1 from ESA (Foing et al., 2006); SELENE Kaguya from JAXA (Namiki et al., 2009); Chandrayaan-1 and 2 from ISRO (Goswami et al., 2011); LRO (Lunar Reconnaissance Orbiter) and GRAIL (Gravity Recovery and Interior Laboratory) from NASA (Schmidt et al., 2012), resulting in many new discoveries and scientific achievements.

China's lunar exploration has been going on for over 13 years beginning with the Chang'e 1 launched in 2007 (Wei et al., 2018; Li et al., 2019). Precise orbit determination technology was first realized and tested on this mission, and was the first step towards follow-up Chinese deep space explorations (Chen et al., 2011). Yan et al. (2010; 2012) systematically analyzed Chang'e 1 orbital tracking data and used these data to solve two lunar gravity models, CEGM01 and CEGM02. The Chang' e 1 also yielded other significant scientific results, including the global image data and a digital elevation model (DEM), as well as a global brightness temperature map of the Moon (Li et al., 2010; Ouyang et al., 2010; Zheng et al., 2012).

The Chang'e 2 spacecraft launched on October 1, 2010, had several goals related to lunar and deep space exploration. During this flyby mission, it conducted 7 m resolution image acquisition from the spacecraft at a height of 100 km to generate a high-resolution global DEM (Ren et al., 2019). The orbit of the spacecraft was adjusted to an ellipsoid orbit, with a perilune height of 15 km and an apolune height of 100 km to collect additional imagery in preparation for the Chang'e 3 lander and rover (Zhou et al., 2011). After Chang'e 2 conducted observation from the 100 km lunar orbit, it traveled to the Sun-Earth Lagrangian point ($\boldsymbol{L_2}$). The Chang'e 2 spacecraft conducted a successful flyby of the near-Earth asteroid 4179 Toutatis, for the first time, providing significant information about the characteristics, formation and evolution of this asteroid from close distance imaging (Huang et al., 2013).

The Chang'e 3 was an unmanned lunar exploration operation incorporating a robotic lander and rover and tested several phase orbit determination scenarios (He et al., 2014; Li et al., 2014). Chang'e 3 was inserted into an initial near circular orbit on December 6, 2013, at a height of 100 km after aerobraking. On December 10, Chang'e 3 entered an elliptical orbit and landed at (19.51W, 44.12 N) northwest of the Mare Imbrium (Li et al., 2015). A soft landing was necessary to protect the rover and lander. This represented a challenge for orbit control and determination. The published results focus on the Chang'e 3 positioning and soft landing of lander and the rover, but little attention has considered the lunar orbit phase. A new kinematic method for lander positioning was proposed and provided by Huang et al. (2012; 2014), meanwhile Klopotek et al. (2019) calculated the Chang'e 3 lander position with the help of the news observations as tracked by the geodetic VLBI. In addition, Liu et al. (2020) used the VLBI delay data from the Chang'e 3 lander and determined its position with a Helmert-VCE-aided weighing method to improve its positioning accuracy further.

China's fourth lunar probe, Chang'e 5T1, was launched on October 23, 2014, tested reentry technology, which is remaining on orbit. Chang'e 5T1 aimed to test the Earth atmosphere reentry technology (Fan et al., 2015). The extended mission after separation included three orbital phases: high eccentric parking orbit, trans-lunar orbit, and a Lissajous trajectory in the vicinity of the Earth–Moon Lagrange point L_2. The probe continued to orbit the Moon with an inclination from 28 degree to 68 degree after concluding the extension mission. Based on its orbital tracking data in 2015 and 2016, Yan et al. (2020) solved a lunar gravity field model CEGM03 up to degree and order 100.

Subsequent to Chang'e 5T1, the Chang'e 4 mission was launched on 7 December 2018, which is a farside lander mission. The goal of Chang'e 4 mission was to explore the Von Kármán crater on the floor of the South Pole-Aitken basin (Wu et al., 2019). This mission contained a relay satellite named Queqiao, a lander and a rover named Yutu-2 (Li et al., 2019). This mission was the first on-site investigation of the lunar farside, thus a soft landing on the lunar farside was a new challenge as there was no possibility of Earth-based radio tracking. In May of 2018, Queqiao, as a part of Chang'e 4 mission, was successfully deployed to the Earth-Moon Lagrange point ($\boldsymbol{L_2}$) to relay communications for farside operations. Liu et al. (2019) reconstructed the landing trajectory and determined the location of the landing site using the combination of data from terrain data and the landing and navigation cameras.

A key technique in all these missions was the acquisition orbital tracking data from the spacecraft. The radio communication system provides accurate measurements with high operational availability, and widely used in the deep space exploration since the last century (Montenbruck et al., 2005). Spacecraft orbit determination relies on Doppler and range measurement from Earth tracking stations (Ellis, 1983). We can obtain dynamic lunar parameters, including spherical harmonic coefficients of the gravity field model, tidal Love numbers, ephemerides, and even the rotation model by analyzing tracking data derived from Precise Orbit Determination (POD). These parameters will significantly help to explain the body shape, tides effect, and deep interior structure of the Moon, as well as its origin and evolution (Zuber et al., 2013; Harada et al., 2014; Goossens et al., 2019). POD accuracy is directly related to the dynamical models used in POD software such as data correction, force, and measurement models used in the data processing and tracking data quality (Tapley et al., 1994).

The radio tracking data quality relies heavily on the deep space tracking networks on Earth. Along with the successful implementation of the Chang'e 3 mission, China has already built a worldwide deep space tracking network that can continuously track spacecraft and provide accurate range and Doppler measurements, which can support future Mars and even Jupiter system missions. The Beijing Aerospace Flight Control Center is the radio tracking data processing center of Chinese deep space missions. They also provide these radio science data to related scientific research group aiming to dig out the science goal.

Although China has launched lunar series missions with engineering and science successes, its progress on spacecraft orbital radio tracking data processing is less well known. In this paper, we focus on the orbit determination in the Chang'e series missions and reprocess the tracking data to summarize the development in orbit determination accuracy. We review the Chang'e series missions, present detailed orbital information and tracking data collection in section 2. In section 3, we explain the orbital tracking data processing and the POD computation environment. We analyze the accuracy of the POD for the Chang'e spacecraft and compare the results to those discussed in other publications in section 4. A brief summary of radio orbital

tracking data processing in the Chang'e missions and future prospects will be included in section 5.

2 Chang'e missions and orbit designs

2.1 Missions orbital geometry description

The orbits design and tracking information will be introduced in this section. By 2020, China had executed five moon explorations, Chang'e 1, Chang'e 2, Chang'e 3, Chang'e 5T1, and Chang'e 4. We illustrate the types of orbits and key flight trajectories in Fig.1.

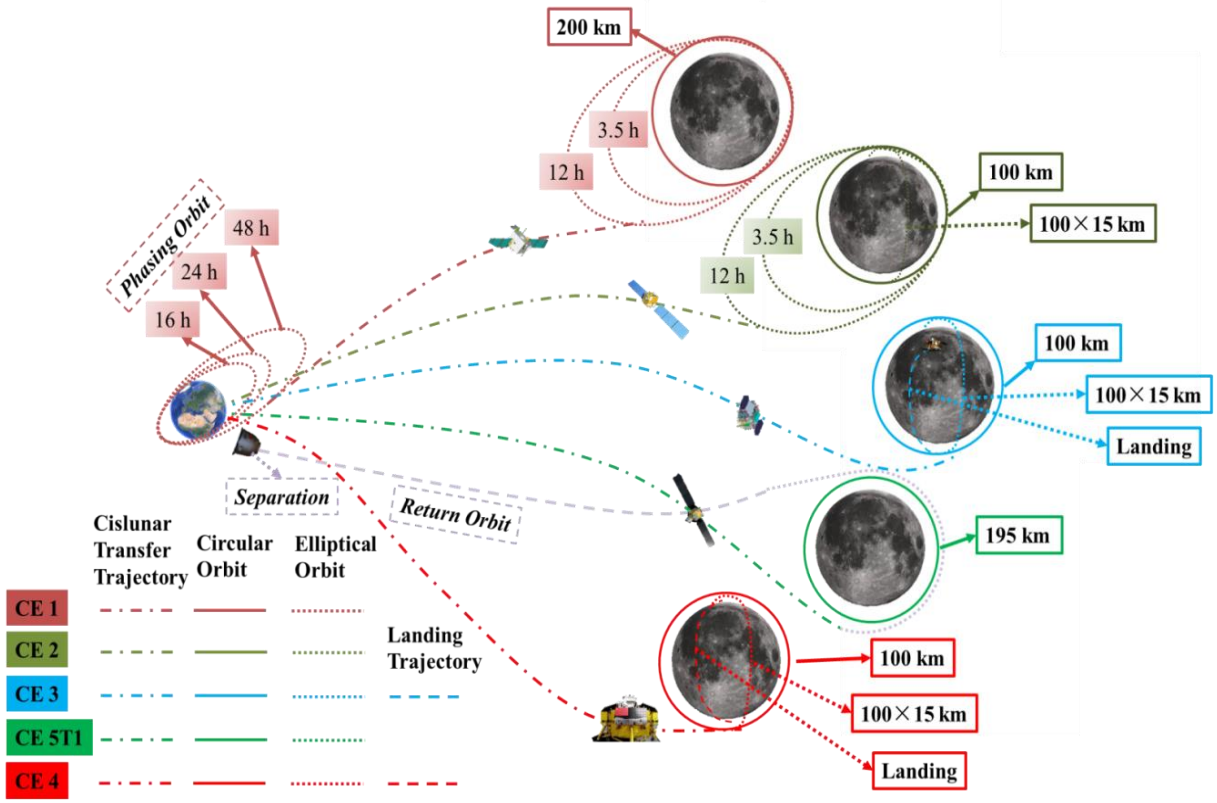

Fig.1 China's past Chang'e series mission and orbits. Different colors represent different mission; different line types indicate different orbit types.

As shown in Fig.1 (the dark red line), the Chang'e 1 entered lunar orbit after a long and complicated journey about 32 hours long with eight orbital maneuvers. On November 5, 2007, in three orbit transfer sequences, the Chang'e 1 spacecraft was inserted into a highly elliptical, near-polar orbit around the Moon with an apolune altitude of 10, 000 km and a perilune altitude of 2, 000 km. It was finally inserted into a near-polar, near-circular orbit with an orbital height of 200 km after three aero-braking maneuvers over the following three days.

Fig.1 (dark green line) depicts how the Chang'e 2 directly injected into the lunar-transfer orbit, without first settling into an Earth orbit. The lunar-transfer orbit journey was about 112 hours. On October 09, 2010, after an earth-moon transfer and braking three times near the moon, the Chang'e 2 spacecraft entered a period of lunar orbiting at a height of 100 km. The spacecraft descended to an orbit with an altitude of 15 km at the perilune point and 100 km at the apolune

point to obtain high-resolution images of the Chang'e 3 landing site. On October 29, it shifted to a circular orbit with a height of 100 km again. On December 13, 2012, Chang'e 2 conducted a successful flyby of the near-Earth asteroid 4179 Toutatis with a closest distance of 770 ± 120 meters from the surface of the asteroid (Huang et al., 2013; Cao et al., 2015). From Fig.1 (blue line), the Chang'e 3 flew directly to the Moon and executed two types of orbits, 100 km × 100 km and 100 km × 15 km.

The green line in Figure 1 shows that the Chang'e 5T1 orbit was quite different from the others previous missions. The Chang'e 5 T1 contained a service module and a return vehicle was separated on October 31 2014. The service module started its extended mission after separation. The extended mission includes three orbital phases, a high eccentric parking orbit, a trans-lunar orbit, and a Lissajous trajectory in vicinity of the Earth-Moon Lagrange point L_2. And then the service module has continued to orbit the moon after the extension mission.

From Fig.1 (red line), we can see the Chang'e 4's orbit is similar as the Chang'e 3 mission, as a landing mission. On January 3, 2019 the Chang'e 4 safely landed on the floor of Von Kármán crater, on the farside of the moon. Queqiao is used to realize the lander and rover to the ground communication. Queqiao adopted a Halo orbit around the Earth-Moon Lagrange point L_2. After the mission orbits analysis, we will introduce the supporting tracking equipment system in next part.

2.2 Spacecraft tracking network

The setting up of a network of tracking and telemetry stations, on one hand, can receive signals from spacecraft, and on the other hands, transmit commands to them to correct the orbits. China's deep space tracking system has gradually built and developed along with the China lunar exploration Program. In this study, we mainly concerned the POD results during orbiting moon phase, which has less maneuvers and is more stable to evaluate the tracking network capability and accuracy. Thus, we did not display some tested skills in tracking phase such as, GPS. Related basic orbital geometry of selected orbits and tracking information for these Chang'e missions are summarized in Table 1.

Table 1: Orbit parameters and tracking configures during orbiting phase

Mission	Height (km)	Eccentricity	Inclination (°)	Band	Tracking stations		
					Kashi	Qingdao	Jiamusi
Chang'e 1 (Ouyang et al., 2010)	200	0	88-91	S-band	×	×	
Chang'e 2 (Chen et al., 2012)	100	0	90	S-/X-band	×	×	
Chang'e 3 (Li et al., 2015)	100	0.015	90	S-/X-band	×	×	×
Chang'e 5T1 (Yan et al., 2020)	195	0.04	18-68	S-/X-band	×	×	×
Chang'e 4	100	0	90	S-/X-band	×	×	×

Note: S-band (Uplink: 2025~2110 MHz; Downlink:2220~2290 MHz); X-band (Uplink: 7145~7235 MHz; Downlink:8400~8500 MHz).

From Table 1, we can see the Chang'e 1 was tracked by a USB (Unified S-Band) system with two antennas located at Qingdao station (with diameters of 10 m and 18 m) and two antennas located at Kashi station (with diameters of 12 m and 18 m). Meanwhile, the VLBI technique was firstly, as a supplement tool, took part in the Chang'e 1 mission tracking and navigation sessions. The Chang'e 2 is the backup mission of Chang'e 1, and the same tracking antennas was used as the Chang'e 1 mission. Especially, the X-band tracking as a key technology was firstly tested in the Chang'e 2 mission.

After Chang'e 2 mission, the antennas capability was significantly improved. Kashi

191 station built a new antenna with a diameter of 35 m and with S/X/Ka bands; Qingdao 18 m S-
192 band only received antennas were upgraded to S/X band full function tracking equipment;
193 Jiamusi station built an antenna with a diameter of 66 m and with S/X bands. The Chang'e 3 is
194 the first mission using the modern China Deep Space tracking, telemetry and command Network
195 (CDSN) and Very long baseline interferometry Network (CVN) together. The CDSN includes
196 two stations at Qingdao, Kashi, and Jiamusi, in China, and one station in Argentina with antenna
197 diameter of 35 m (the first oversea deep space station). The CVN includes four stations at
198 Urumqi (25 m antenna), Kunming (40 m antenna), Beijing (50 m antenna) and Shanghai (65 m
199 antenna).
200 The CDSN not only can further support effective tracking coverage of future lunar,
201 Mars and asteroids missions, but also even can meet requirement for the implementation of the
202 whole solar system exploration (He et al., 2020). The radio science data were made available
203 both to its in-house staff and to visiting scientists who wished to use them to analyze and study
204 the moon science.

205 **3 POD setting**

206 3.1 POD software

207 We adopted our in-house software, LUGREAS, to do POD for the series of Chang'e
208 missions. LUGREAS was written in Fortran 90 and designed to be a comprehensive and flexible
209 system for executing POD as well as estimating dynamic parameters to investigate the interior
210 structure of the moon (e.g., Yan et al. 2016, 2020). We have strictly validated LUGREAS
211 software with GEODYN II (Pavlis 2001; Ye et al., 2016). It has been extended to analyze orbital
212 tracking data from various missions targeting different planetary bodies such as Mercury (e.g.,
213 Yan et al. 2019), Mars (e.g., Yan et al. 2018; Yang et al.,2020), and asteroids (e.g., Jin et al.
214 2020). LUGREAS can accomplish the following tasks,
215 (i) Effectively predicts the spacecraft trajectory including all the perturbation force models;
216 (ii) Generates simulated tracking data. LUGREAS supports simulation of tracking data from
217 one or two earth stations, e.g., one-way range-rate, two-way range/range-rate, three-way
218 range/range-rate, VLBI delay/delay rate, same-beam VLBI, and four-way Doppler.
219 (iii) Supports spacecraft POD, precise positioning of lunar lander, k_2 solution, and lunar
220 gravity field recovery through the Bayesian least squares method.
221 The detailed software structure and its applications for processing the Chang'e 5T1
222 mission can refer these publication (Yan et al., 2020; Liu et al., 2020). In this study, we will
223 firstly use LUGREAS to process the radio tracking data from Chang'e 1 to Chang'e 4 together,
224 which provide a view to review the mission tracking feasibility, systematically.

225 3.2 Computation configurations

226 In this section, we will describe the software parameter settings. For POD, we
227 estimated the initial orbital elements of spacecraft per arc and if necessary, we estimated the
228 empirical acceleration to compensate for un-modeled force. Pass-dependent biases in the two-
229 way Doppler/range were estimated to account for measurement modeling error. The arc length
230 was set to one day, depending on the unrecorded time of the momentum wheel action during
231 spacecraft tracking. The detailed configurations for POD, including the dynamic models,
232 correction models, estimated parameters, and other models, are listed in Table 2.
233

234 **Table 2:** Configurations for POD and gravity field recovery in LUGREAS.

	Types	Details
Dynamic model	**A priori gravity field**	SGM100h (Matsumoto et al., 2010), CEGM02 (Yan et al., 2012), or GRGM660 (Lemoine et al., 2013)
	N-body perturbation	Sun and eight planets from JPL DE421 (Willimas et al., 2008)
	Lunar solid tidal perturbation	k_2=0.0240 (Love Numbers from Matsumoto et al., 2010)
	Perturbations from Earth-Moon oblateness	Moon J2 indirect perturbation; Earth J2 perturbation
	Relativity perturbation	Schwarzschild (Sun only)
	Solar radiation	Fixed ratio of area to mass (pressure coefficient: 1.2)
Correction model	**Relativistic acceleration correction**	Moyer (2003)
	Earth tropospheric correction	Hopfield model (Hopfield 1963) + CfA2.2 mapping function (Davis et al., 1985)
Others	**TDB-TT translation model**	Moyer (1981)
	Tracking station correction	Earth solid tide, ocean tide and polar tide correction
	Earth rotation model	IAU 2000 precession-nutation (Seidelmann et al., 2007); Polar motion parameters from IERS C04
	Moon rotation model	JPL DE421 (Williams 2008)
	Data and weighting	Two-way Doppler with fixed weight 1cm/s; Range with 5 m
	Ephemeris	JPL DE421 (Willimas 2008)
	Estimated parameters	Initial orbit values; empirical accelerations; S-band bias

235

236 In Table 2, the force models include a lunar gravity field, N-body perturbations,
237 perturbations stemming from the Earth-Moon oblateness, relativity perturbations, solid tidal
238 perturbation, and solar radiation. The force and measurement models used in this analysis refer
239 the previous tracking data processing work in Chang'e missions (Yan et al., 2010, 2012, 2020).
240 Relativistic acceleration correction was used in the perturbation calculations when integrating the
241 spacecraft orbit. The Earth tropospheric correction and tracking station coordinate correction
242 were adopted in the theoretical observation calculations.
243 Besides, others models used in POD has been concluded here. The Earth-fixed
244 coordinate system and the locations of the tracking stations were adopted to be consistent with
245 the terrestrial reference frame ITRF2014 recommended by the International Earth Rotation
246 Service (Bizouard et al., 2019). The Lunar-fixed coordinate system was chosen to be consistent
247 with the orientation parameters of the JPL DE421 planetary ephemeris (Willimas 2008), and so
248 were the ephemerides of the Sun, the Earth and other planets. The inertial coordinate system
249 used for orbit integration was the lunar-centered inertial coordinate system J2000. The initial
250 orbital elements were retrieved from a reconstructed initial ephemeris of Chang'e series
251 spacecraft provided by Beijing Aerospace Control Center. The lunar gravity field models are
252 truncated to degree and order 100 for these three models in POD processing.
253 As we pointed out, although these missions vary each other in orbital design character,
254 in the following sections we only focus on the circle or ellipse orbits, which are relatively stable
255 with less artificial controls to elevate the orbit accuracy. We only focus on the range data or
256 Doppler data from CNSD, which was processed with LUGREAS to review the development of
257 radio measurement accuracy in Chinese lunar exploration missions. Normally, the Doppler data
258 were sampled at 1 s intervals during the series of Chang'e missions. For different missions, there
259 exists a small difference in the tracking data strategy, so the related processing strategy will be
260 further clarified in the result sections of this paper.
261 Based on these parameters settings, the orbit determination results and the orbit
262 accuracy evaluation are presented in the next section. Since the real position of the Chang'e

series spacecraft is unknown, our estimation results were assessed by tracking data residuals analysis, short arc POD analysis, and orbital overlap statistics.

4 POD results and discussion

4.1 Chang'e 1 mission

The tracking data from December, 2007 to November, 2008 were analyzed for Chang'e 1 mission to evaluate the orbit accuracy. This period contains the orbiting moon phase, where the spacecraft was in a near-polar, and the near-circular orbit phase with an orbit height of 200 km.

Since Qingdao and Kashi stations were in charge of tracking the Chang'e 1 spacecraft, only one station could observe the spacecraft at a time point, which limited the amount of the obtained observations. Moreover, since the unloading and uploading maneuvers were frequently performed at the farside of the moon, the tracking data for the arc length was limited to less than 10 hours. Thus, each of the daily orbits were divided into two arcs.

In the POD procedure, the two-way range and Doppler data were weighted with 5 m and 1 cm/s. There was a significant systematic bias about 2 cm/s in the Doppler data, so its sigma was set at a value larger than the actual observational accuracy. The systematic bias was mainly induced by drift of local oscillation of the clock in the tracking station, and could be removed through orbit determination.

In this work we choose three typical gravity field model, SGM100h from SELENE mission, CEGM02 from Chang'e 1mission, and GRGM660 from GRAIL mission. Three typical gravity field models (calculated by JPL, JAXA, and our research group) were used in data processing. The precision of lunar satellite orbit determination depends on the quality of the lunar gravity field model, since gravity is the dominating perturbing force acting on the satellite. Considering different gravity models, on one hand, the POD results based on different gravity models could be crossed verified each other; on the other hand, we can evaluate the accuracy of different lunar gravity models through POD. We processed 198 arcs, and the RMS of range and Doppler residuals of the arcs were listed in Table 3.

Table 3: Residuals RMS of Chang'e 1 based on three lunar gravity models

Year	Arc	Two-way Doppler (mm/s)			Two-way Range (m)		
	Number	SGM100h	CEGM02	GRGM660	SGM100h	CEGM02	GRGM660
07-12	17	1.081	1.078	1.081	2.096	1.955	2.054
08-01	21	1.037	0.696	0.973	2.047	2.253	2.094
08-02	10	0.418	0.546	0.428	1.682	1.760	1.696
08-05	22	1.716	1.650	1.716	1.886	1.897	1.885
08-06	21	2.059	1.903	2.105	1.495	1.472	1.505
08-07	26	1.589	1.681	1.589	1.592	1.628	1.595
08-08	23	0.674	0.563	0.676	1.302	1.285	1.408
08-09	23	0.203	0.189	0.192	1.038	1.037	1.037
08-10	23	0.406	0.315	0.416	1.107	1.092	1.108
08-11	12	1.515	1.515	1.515	1.585	1.580	1.587
Mean		1.070	1.070	1.014	1.069	1.583	1.596
RMS		0.603	0.603	0.599	0.611	0.345	0.369

From the monthly mean values of residuals RMS as presented in Table 3, we can see that there is a close consistency in the distribution trend of orbital residuals of the two-way Doppler and range between the gravity models. For different months, the RMS of residual changes from about 0.2 mm/s to 2.1 mm/s for the two-way Doppler and from about 1.0 m to 2.3 m for the two-way range. Since the radiometric tracking using S-band was done by single-

frequency downlink, the accuracy was heavily affected by the ionosphere and solar plasma. Meanwhile, Yan et al. (2010) analyzed the range and Doppler data and the accuracies of range and Doppler was reported as 2 m and 1 mm/s.

Moreover, when we processed the data we found that some arcs have the large residuals, which does not reflect on the monthly average residuals RMS directly. We inferred that it corresponds to a large satellite attitude adjustment or a phase when the satellite orbital plane was approximately perpendicular to the observation direction of the earth tracking station (see Fig.3 (a)), which is insensitive for calculations of the spacecraft orbit.

Taking 07-12 case for instance, Fig.3 (b) shows the observation angle change during December 2007. The period marked by a blue box indicates the highest observing angle, where the corresponding residuals RMS (1.55 mm/s for SGM100h, 1.50 mm/s for GRGM660, and 1.48 mm/s for CEGM02) were far larger than 1.081 mm/s.

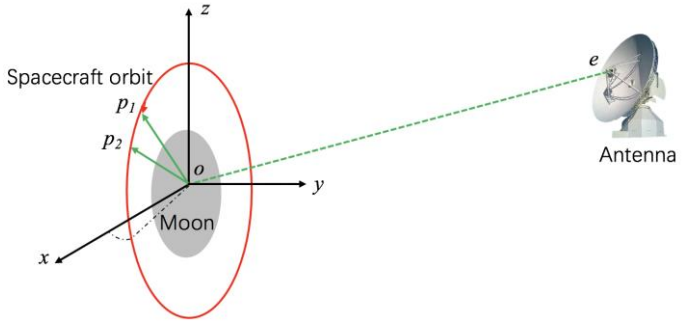

(a) View geometry

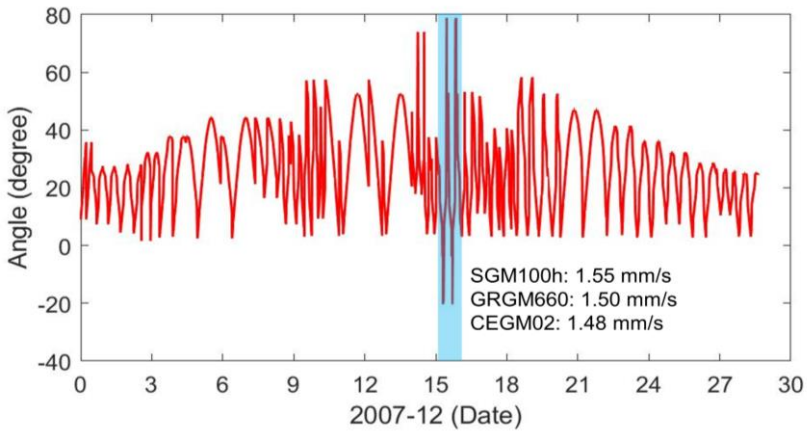

(b) Observing angle

Fig. 2 View geometry and observing angle. P_1 and P_2 are points on spacecraft orbit. The angle between the orbit plane $\boldsymbol{P_1\text{-}O\text{-}P_2}$ and the observing vector $\boldsymbol{EO}$ defines as the observing angle to distinguish the face-on orbit (with angle of 0°) and edge-on orbit (with angle of 90°). When the angle is closed to 90 degree, the observation is not sensitive for the orbit determination calculation.

To assess to orbit accuracy, we analyzed the RMS of orbital overlaps difference. The orbital overlaps mean that we extended one-day arc constrained by observations by six hours (unconstrained) to compare them with the neighboring one-day (constrained) arcs. We selected the whole month of December of 2007 as the comparative arcs. The numerical results of nine overlaps are listed in Table 4. The overlap errors were presented in the RTN coordinates frame.

Three strategies, based on the SGM100h, CEGM02, and GRGM660, separately in the POD also were used based on all of the available two-way range and Doppler data.

Table 4: RMS of orbital overlap errors in radial (R), normal (N), and tangential (T) directions (m)

	SGM100h				CEGM02				GRGM660			
Arc	R	N	T	Position	R	N	T	Position	R	N	T	Position
1	3.58	-618.32	0.28	618.33	3.65	-606.07	0.26	606.08	3.54	-616.48	0.30	616.49
2	4.21	-131.32	-0.01	131.38	3.41	-210.50	0.30	210.53	4.25	-128.70	-0.03	128.77
3	8.12	-81.10	2.78	81.55	8.51	-48.43	4.56	49.38	8.24	-79.25	2.66	79.72
4	2.09	373.61	9.85	373.74	2.03	343.58	9.12	343.70	2.11	363.78	9.61	363.91
5	6.89	-269.72	-2.15	269.82	6.84	-280.07	-2.26	280.16	6.88	-273.04	-2.19	273.14
6	7.53	-124.30	-0.09	124.53	7.43	-125.53	-0.09	125.75	7.57	-127.76	-0.10	127.98
7	3.72	-175.75	1.92	175.80	2.71	-386.90	5.68	386.95	3.66	-187.47	2.14	187.52
8	11.94	-128.20	5.27	128.86	11.18	-156.35	4.33	156.81	11.94	-128.30	5.26	128.96
9	6.22	-307.95	-0.25	308.01	6.26	-310.14	-0.29	310.20	6.19	-299.42	-0.24	299.49
RMS	3.01	259.39	3.65	170.64	3.05	260.85	3.68	165.62	3.03	256.19	3.59	168.52

From Table.4, we can see that the overlap differences have a very slight improvement with the help of the GRGM660 models with respect to the SGM100h and CEGM02 model. A similar accuracy in Yan et al (2010) about 231.12 m was observed. Moreover, Chen et al. (2011) compared their reconstructive orbit with the ephemeris of Chang'e 1 spacecraft from GEODYN II and concluded that the relative deviation of the orbit determination is at the100 meter level and tens of meters for orbiting lunar phase with respect to the orbit determination results obtained by GEODYN II. This deviation however reflected the difference of measurement model, forces model, and reference system between of two software, and cannot indicate the real orbit determination accuracy.

4.2 Chang'e 2 mission

Orbit determination for 36 arcs was performed during the regular Chang'e 2 management period from October to December 2010. Some of these arcs were intermittent as there were too few observations to determine the orbit or experienced significant orbital adjustment. The observations are provided by the stations of Kashi and Qingdao, and the length of the orbital arc segment is 24 hours.

In the POD procedure, the two-way range and Doppler data were weighted by 5 m and 1 cm/s, respectively, but the range observation data was only available for October however, and the residuals RMS was about two meters. We also reprocessed the tracking data based on three gravity field models. The RMS of range and Doppler residuals of these 36 arcs are summarized in Table 5.

Table 5: Residuals RMS of Chang'e 2 based on three lunar gravity models

Arc	Two-way Doppler (mm/s)			Two-way Range (m)		
Number	SGM100h	CEGM02	GRGM660	SGM100h	CEGM02	GRGM660
October (10)	0.283	0.249	0.241	2.403	2.028	2.070
November (21)	0.263	0.270	0.258		-	
December (5)	0.215	0.172	0.171			
Mean	0.254	0.230	0.223			

Table 5, shows that using the X-band in the tracking system significantly improved the accuracy of Doppler measurements. The tracking accuracy was at least five times that of Chang'e 1 mission. We can see using GRGM660 model the observations can be fitted better than

using CEGM02 and SGM100h when processing Doppler data. The statistics of the overlap difference are listed in Table 6. The overlap length was set as 6 hours and 12 overlaps were collected.

Table 6: RMS of orbital overlap errors (m)

	SGM100h				CEGM02				GRGM660			
Arc	R	N	T	Position	R	N	T	Position	R	N	T	Position
1	16.40	-1.61	119.36	120.49	41.91	43.04	8.53	60.68	-1.89	-4.23	-30.55	30.90
2	5.11	-48.55	-0.07	48.82	-8.78	3.56	-47.70	48.63	3.72	-157.97	3.24	158.05
3	8.85	8.28	1.39	12.20	62.13	42.96	4.06	75.64	6.01	-9.06	1.58	10.98
4	1.27	33.85	-13.15	36.33	8.34	40.30	-0.95	41.16	2.41	-74.57	9.03	75.15
5	-38.05	-195.19	12.30	199.24	6.04	30.07	-3.24	30.84	-7.97	82.68	-265.85	278.53
6	12.13	44.78	-143.01	150.34	-11.16	60.64	13.08	63.03	-0.03	370.85	-25.35	371.71
7	2.52	165.35	-71.46	180.15	19.08	-36.03	-83.67	93.08	0.01	-145.08	89.22	170.32
8	-32.55	162.88	394.35	427.90	-14.34	-239.68	-39.86	243.39	8.13	469.19	-234.00	524.37
9	7.97	17.38	-28.75	34.53	3.06	71.21	-82.62	109.11	-92.50	-156.86	-4.92	182.17
10	-93.50	484.07	-13.35	493.20	5.90	-479.64	-535.04	718.58	-3.58	136.30	24.54	138.54
11	-0.39	-498.85	-119.64	513.00	18.09	-239.94	-2.45	240.64	1.30	-199.98	-70.43	212.03
12	1.44	266.12	197.02	331.12	-14.56	514.82	-45.53	517.03	-3.07	154.15	274.42	314.76
RMS	31.42	240.42	147.84	184.08	23.28	238.07	151.03	217.63	27.19	214.28	138.69	147.85

From Table 6, comparing the results using the SGM100h and CEGM02 models, the differences in three directions decreased when the GRGM660 model was employed for POD, especially in the normal direction of the orbital plane.

These results agree with the orbit accuracy evaluations Chang'e 2 from other researching centers, Beijing Aerospace Flight and Control Center and Shanghai Astronomical Observatory. Chen et al. (2012) adopted long arc orbit determination and estimated the orbit accuracy of the Chang'e 2, about 100 m, based on the combined data, Doppler, range and VLBI data. Li et al. (2012) also did a detailed overlapping analysis for Chang'e 2's 100 km×100 km lunar orbit and for 15 km×100 km orbit based on range and VLBI delay and delay-rate data. They found the VLBI data improves the orbit overlapping to a great extent when the angle between the Earth-Moon vector and the Nominal vector of the orbital plane, where the total difference improved from 123 to 31 m.

4.3 Chang'e 3 mission

For a successful Chang'e 3 lander mission, the spacecraft orbits had to be designed to approach the moon gradually. During the Chang'e 3 orbiting moon phase, the orbit height was 100 km with an eccentricity of 0.015. To prepare for the landing, the Chang'e 3 spacecraft implemented a descending orbit to adjust the altitude of the near moon orbit at a height of 15 km. The observations for Chang'e 3 spacecraft only provide the range data. In the POD procedure, the range data were weighted by 1 m. To display the orbit accuracy at different orbiting periods, we processed tracking data for two typical periods, a four-day period of circular orbits and a two-day period of elliptical orbits. The responding Doppler data were not included because of its abnormal accuracy about centimeter per second. The postfit residuals after POD is plotted in Fig.3 and Fig.4.

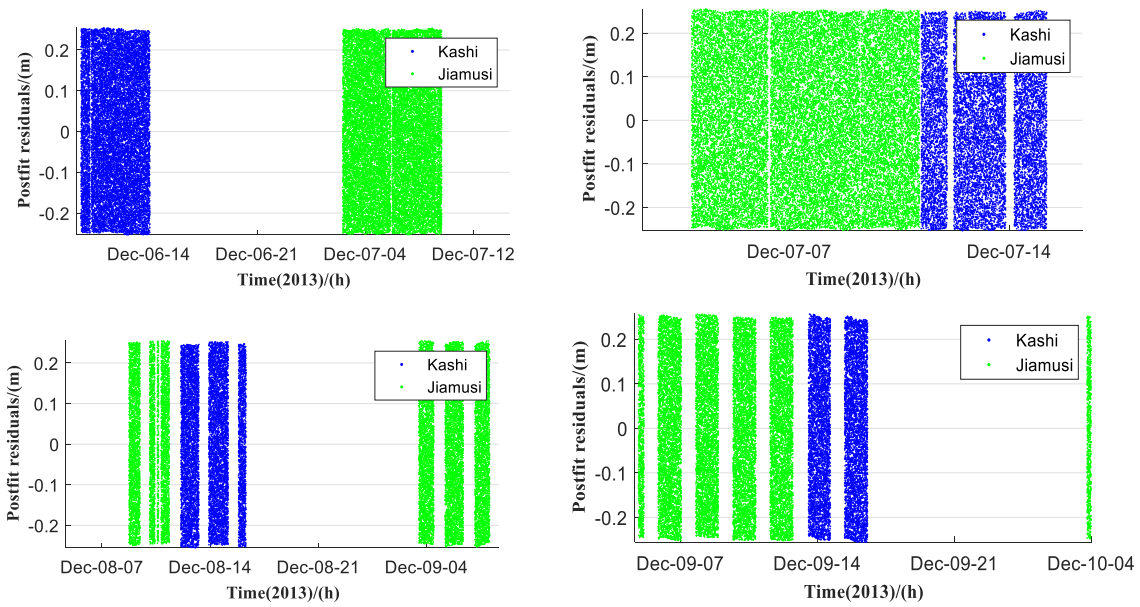

Fig.3 Post-fit residuals at 100 km×100 km orbit (based on CEGM02)

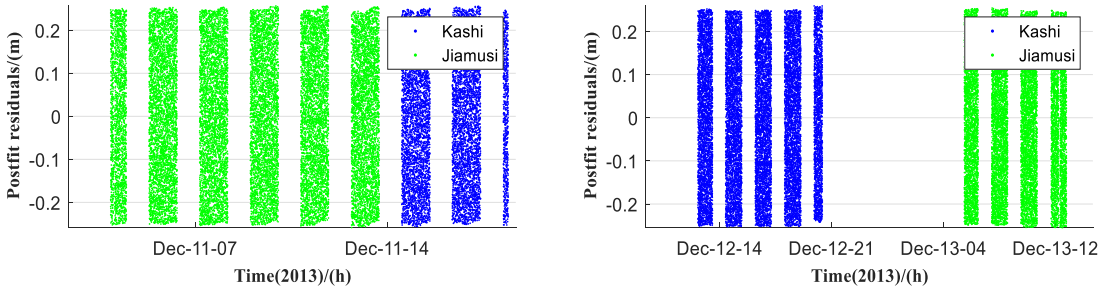

Fig.4 Post-fit residual at 100 km×15 km orbit (based on CEGM02)

From Fig.3 and Fig.4, there is no trend in the residuals, which indicates a high quanlity tracking level. The residual values are listed in Table 7. The range of the residuals is about 0.15 m, which is far smaller than the values of the Chang'e 1 and Chang'e 2 mission, which were about a meter.

Table 7: Range residuals RMS of Chang'e 3 based on three lunar gravity models (m)

Tracking arc (2013)	SGM100h	CEGM02	GRGM660
Dec-06	0.1442	0.1445	0.1439
Dec-07	0.1443	0.1442	0.1444
Dec-08	0.1445	0.1447	0.1443
Dec-09	0.1449	0.1451	0.1447
Dec-11	0.1447	0.1446	0.1447
Dec-12	0.1442	0.1444	0.1440

Furthermore, we have to discussed an interesting residuals mystery a bit in the data processing, that there is no 'horseshoe' trend in the post-fit residuals, which ever happened at Chang'e 1 and 2 circle orbits phase (see Fig. 5). We also could see this phenomenon in papers 10 years ago for Chang'e 2 (Li et al., 2012; Chen et al., 2012), but the reasons never be reported. Here, from the parallel comparison view, we propose the improvement of the residual due to the

modern tracking system, since Chang'e 3 is the first mission using the modern China Deep Space Tracking Network.

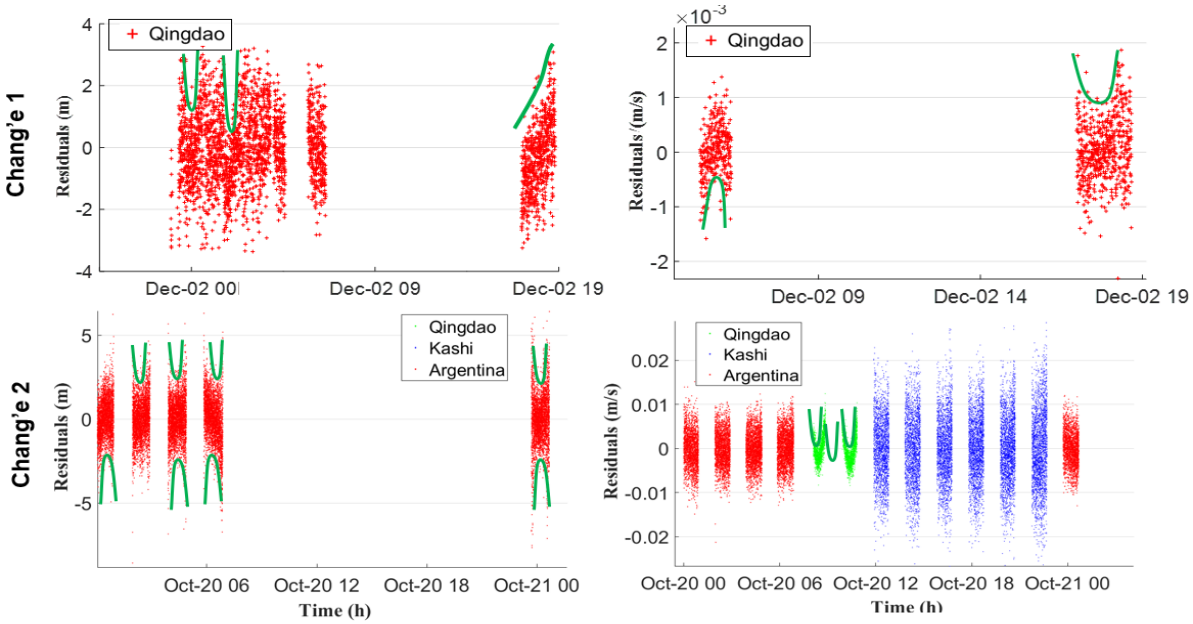

Fig.5 Post-fit residual at Chang'e 1 and Chang'e 2 (based on CEGM02). The green curve fits the 'horseshoe' trend, which only happened at these two missions. This phenomenon also confirmed by tracking data processing center (Private communication, Beijing Institute of Tracking and Telecommunications Technology, 2019; Li et al., 2012).

The orbit determination accuracy of the 100 km×100 km (see Fig.6 (a) and (b)) and 100 km×15 km (see Fig.6 (c)) orbits were evaluated using the overlap orbital differences. The length of the overlap arc was set to six hours.

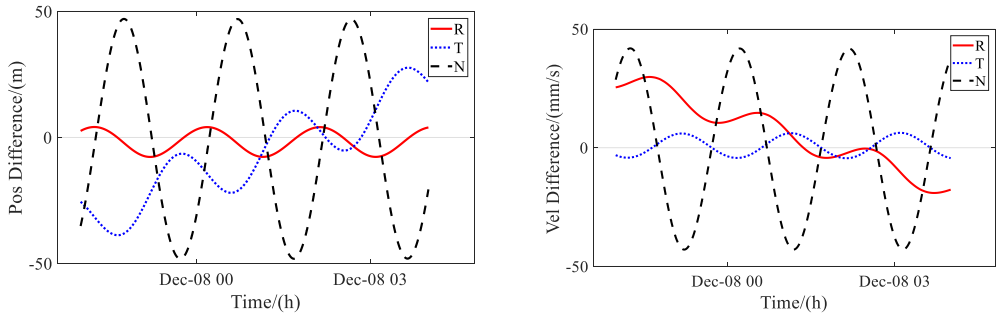

(a) 2013-12-07 and 2013-12-08

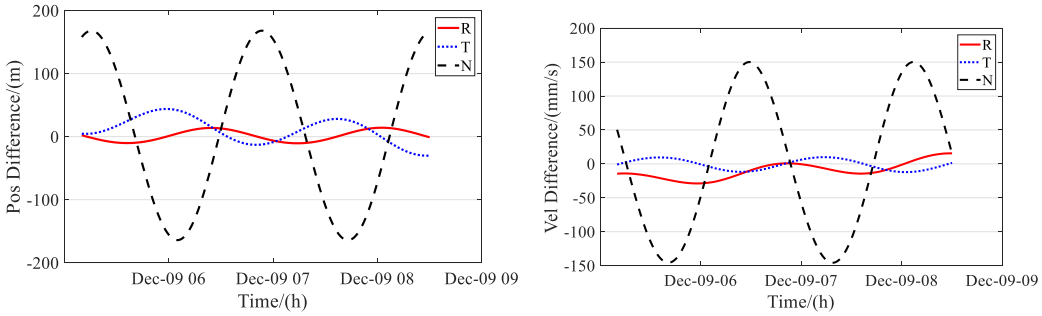

(b) 2013-12-08 and 2013-12-09

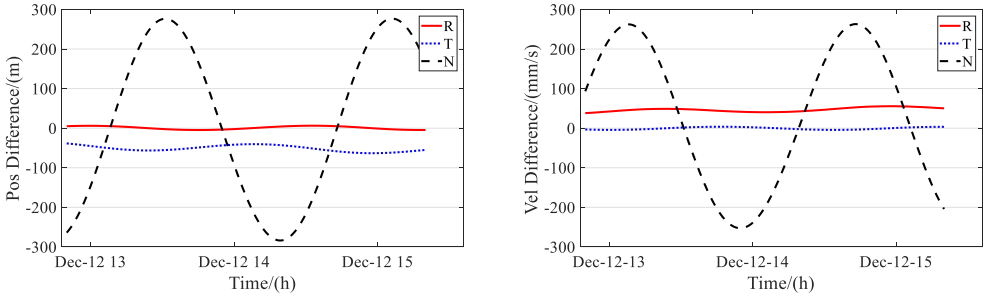

(c) 2013-12-11 and 2013-12-12

Fig. 6 Orbit overlaps difference (based on CEGM02)

From Figs.6 (a) and, (b) and (c), we can see the overlap error was about 50 m to 300 m. Because of the orbit evolution, the Chang'e 3 gradually changed from face-on orbit to edge-on orbit. The orbit overlaps based on three different gravity models are listed in Table 8.

Table 8: RMS of orbital overlap errors (m)

	SGM100h				CEGM02				GRGM660			
Orbits	R	T	N	Position	R	T	N	Position	R	T	N	Position
100 ×100	4.208	18.657	33.499	38.574	3.153	20.108	33.499	39.198	3.236	13.214	24.675	28.177
	8.508	20.238	118.478	120.495	12.785	30.279	130.768	134.835	10.789	12.109	80.326	81.947
100 ×15	3.932	7.409	197.213	197.391	5.231	9.637	172.182	172.531	1.601	3.072	143.451	143.493

From Table 8, we can see for the circle orbit, there has a slight difference on overlap between SGM100h and CEGM02 model, whose mean value of the position difference is about 80 m and 87 m, respectively. Both of them are less accurate than using GRGM660 model about 55 m. It should be noted that, for elliptic orbit phase, using CEGM02 the orbit difference is obvious smaller than SGM100h model, and both of them are still bigger than the difference value obtained from GRGM660 model.

Huang et al (2014) however, processed range and VLBI orbit phase data together. The results show that the orbit accuracy of 100 km×100 km and 100 km×15 km was about 20 and 30 m with 2-hour overlap. This indicates adding VLBI data improved the accuracy of the Chang'e spacecraft overlap results, outperforming calculations using range observations alone.

4.4 Chang'e 5T1 mission

Chang'e 5 T1 tracking data was collected from May 20, 2015 to July 20, 2015 for POD and the orbit accuracy evaluated. The tracking stations were Qingdao, Kashi, and Jiamusi, detailed information about the stations was presented in Section 2.2. We took 14 arcs to analyze

the orbital determination accuracy using the Doppler data. The arc length for POD was set to 24 hours. The post-fit residual of Doppler data is listed in Table 9. These data show that the Doppler accuracy can reach 0.3 mm/s.

Table 9: Doppler residuals RMS of Chang'e 5T1 based on three lunar gravity models

Arc	Two-way Doppler (mm/s)		
	SGM100h	CEGM02	GRGM660
1	0.28	0.54	0.28
2	0.20	0.17	0.17
3	0.51	0.49	0.39
4	0.29	0.21	0.26
5	0.31	0.27	0.24
6	0.45	0.57	0.44
7	0.42	0.46	0.50
8	0.34	0.30	0.31
9	0.18	0.18	0.18
10	0.24	0.24	0.23
11	0.25	0.29	0.46
12	0.49	0.71	0.56
13	0.17	0.17	0.21
14	0.58	0.35	0.17
Mean	0.34	0.35	0.31
RMS	0.13	0.17	0.13

From Table.9, we can see the gravity models have weak influence on the residual. However, the residual is about 0.35 mm/s level, which improved a lot with respect to former missions. The orbit overlaps results are presented in Table 10.

Table 10: RMS of orbital overlap errors (m)

	SGM100h				CEGM02				GRGM660			
No.	R	T	N	Position	R	T	N	Position	R	T	N	Position
1	1.58	6.33	113.60	113.79	6.32	4.95	204.26	204.42	1.44	1.76	100.40	100.42
2	3.23	8.97	234.09	234.29	14.04	19.95	365.07	365.89	2.46	4.14	85.78	85.91
3	12.27	12.05	85.53	87.24	11.91	15.05	49.27	52.88	1.88	1.68	11.66	11.93
4	4.50	3.21	81.44	81.63	7.77	14.54	85.17	86.75	1.50	2.08	10.11	10.43
5	2.69	5.74	83.48	83.72	0.15	0.59	8.89	8.91	0.79	3.33	2.88	4.47
6	6.44	16.23	18.14	25.18	4.11	17.56	7.97	19.72	0.35	2.10	3.10	3.76
7	4.23	5.36	48.62	49.09	10.40	24.83	64.72	70.09	1.45	1.71	10.92	11.14
8	11.37	13.91	118.12	119.48	7.41	5.97	28.17	29.73	0.93	0.56	38.10	38.11
9	3.12	10.27	6.81	12.71	1.67	5.15	32.57	33.02	4.67	7.42	17.51	19.58
10	2.55	1.62	360.15	360.17	2.06	2.44	292.68	292.70	0.35	2.53	155.14	155.16
11	0.36	1.30	28.89	28.92	0.98	2.91	36.81	36.94	1.07	2.58	4.34	5.16
12	3.16	11.52	39.31	41.08	3.15	6.04	22.29	23.31	1.95	0.96	42.10	42.16
13	5.90	11.37	76.93	77.99	2.71	10.10	36.84	38.30	2.88	2.11	32.22	32.42
RMS	3.55	4.75	97.60	96.55	4.45	7.63	116.36	115.38	1.17	1.73	46.66	46.36

From Table 9, we can see that based on the GRGM660 gravity model, the orbit has higher accuracy than the SGM100h and CEGM02 models. The RMS value of the orbit overlap difference based on the GRGM660 gravity model was about 46 meters, which agrees with our earlier processing results (Yan et al. 2020). The whole process on data collected from May of 2015 to December of 2016 can be read in Yan et al. (2020).

4.5 Chang'e 4 relay satellite

We processed the tracking data from the Queqiao relay satellite for the period 5 August to 26 August 2018. This satellite provided continuous relay communications between Earth and the lander on the far side of the Moon; and was deployed in a halo orbit around the Earth–Moon

L_2 point, at about 65,000 km distance from the moon. Thus, its orbit was stable with less maneuvering action. We took 7 day as an arc. During this period, the tracking data is two-way range, and no Doppler data was available. The post-fit residual of two-way range are plotted in Fig.7.

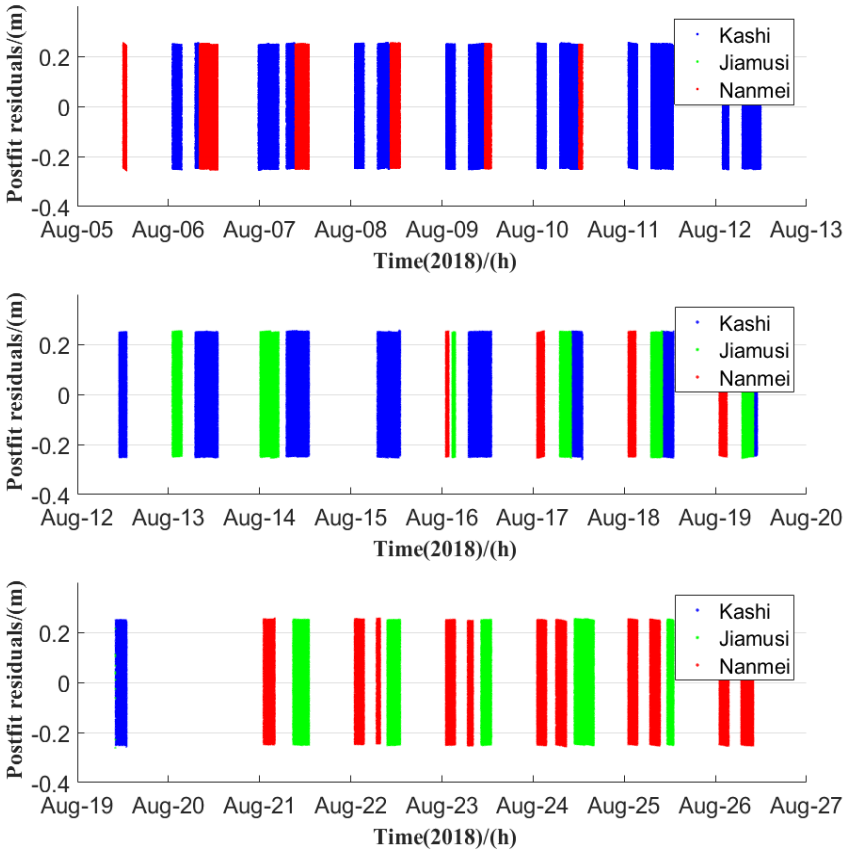

Fig.7 Post-fit residual based on CEGM02

From Fig.7, we can see that the residuals figure is similar as the Chang'e 5T1. The residual information further is listed in Table 11.

Table 11: Two-way range residuals RMS of Chang'e 4 relay satellite based on three lunar gravity models (m)

Arc	SGM100h	CEGM02	GRGM660
1	0.146	0.145	0.144
2	0.221	0.217	0.201
3	0.220	0.217	0.202
Mean	0.196	0.193	0.182
RMS	0.043	0.042	0.033

We can see that the residuals using SGM100h and CEGM02 model are close. We think that since the orbit of relay satellite is far from the moon, the lunar gravity model had less influence on the relay satellite than the traditional Chang'e orbiters. The overlap differences based on SGM100h, CEGM02, and GRGM660 are included in Table 12.

Table 12: RMS of orbital overlap errors (m)

	SGM100h				CEGM02				GRGM660			
No.	R	T	N	Position	R	T	N	Position	R	T	N	Position

1	0.201	0.509	0.572	0.792	0.167	0.439	0.562	0.732	0.167	0.439	0.543	0.718
2	0.112	0.045	0.153	0.195	0.071	0.037	0.104	0.131	0.063	0.025	0.097	0.118
RMS	0.063	0.328	0.296	0.422	0.068	0.284	0.324	0.425	0.074	0.293	0.315	0.424

From Table.12, the results for different three gravity models are almost the same, where the position difference was less than 1 meter. We think there are two reasons. On one hand, the Queqiao around L_2 point and its orbit is stable; on the other hand, the perturbation from the Moon is much weaker because the satellite is far away from the Moon. Qin et al. (2019) adopted 10-degree lunar gravity model and obtained a satisfactory result without obvious systematic trend errors in the residuals. This further demonstrates that the high-degree lunar gravity model's effect could be ignored. Qin et al. (2019) evaluated the orbit precision of the Chang'e 4 relay satellite, finding that the residual RMS for ranging, Doppler, VLBI delay and VLBI delay rate based on S-band, were about 0.53 m, 0.37 mm/s, 1.16 ns and 0.67 ps/s, respectively.

5 Conclusions

The Chinese lunar exploration program has completed five missions and six launches, accumulating a large amount of measured data. The accuracy of POD for lunar spacecraft has continuously improved as tracking ability has developed and matured. The accuracy of range data has improved gradually, from 1.58 m (Chang'e 1) to 0.2 m (Chang'e 4). Chang'e-1 mainly relies on the two-way range data, since the Doppler data quality is unstable. From Chang'e 2 mission, the Doppler data accuracy has gradually improved, from 1.1 mm/s (Chang'e 2) to 0.35 mm/s (Chang'e 5T1). For Chang'e 5T1, POD can be executed, using only Doppler data. Moreover, for Chang'e 4 relay satellite, the POD accuracy was at the meter level.

The downlink/uplink capability of CDSN will be further improved. Follow-up China lunar exploration program Chang'e 6/7/8 will conduct a comprehensive exploration on the South Pole of the Moon and will establish a base on this region. For these missions four-way tracking will possibly be implemented with a link from the CDSN->lunar spacecraft->lander, for lander positioning and selenophysical parameter solutions. We can look forward to seeing more fruitful radio science results from China's future lunar exploration missions.

Acknowledgement

We are grateful to the hard work of Chang'e mission team to make this research possible. NASA is appreciated for providing models and ephemeris in our research. This work is supported by National Scientific Foundation of China (U1831132, 41874010, 41804025), Innovation Group of Natural Fund of Hubei Province (2018CFA087). The BSP file of the orbit of Chang'e series missions are available by contacting the corresponding author.

Data Availability Statement

Data for this research are not publicly available due to policy of China space agency, but available to researchers with appropriate credentials. The LUGREAS software used in this analysis is proprietary to Wuhan University; however, the processing of the observables and estimation procedure is given in Yan et al., 2020.

Reference

Binder, A.B. (1998). Lunar prospector: overview. Science, 281(5382), pp.1475-1476.

Bizouard, C., Lambert, S., Gattano, C., Becker, O., &Richard, J.Y. (2019). The IERS EOP 14C04 solution for Earth orientation parameters consistent with ITRF 2014. Journal of Geodesy, 93(5), pp.621-633.

Cao, J., Liu, Y., Hu, S., Liu, L., Tang, G., Huang, Y., & Li, P. (2015). Navigation of Chang'E-2 asteroid exploration mission and the minimum distance estimation during its fly-by of Toutatis. Advances in Space Research, 55(1), 491-500.

Chen, M., Tang, G.S., Cao, J.F., Zhang, Y. (2011). Precision Orbit Determination of CE-1 Lunar Satellite. Geomatics and Information Science of Wuhan Universit, 36(2), pp.212-217.

Chen, M., Zhang, Y., Cao, J.F. (2012). Orbit determination and tracking technology of CE-2 satellite (in Chinese). Chin Sci Bull, 57: 689–696. Doi: 10.1360/972011-818

Crawford IA. (2012). The scientific legacy of Apollo. Astron. Geophys., 53, 6.24-6.28. Doi: 10.1111/j.1468-4004.2012.53624.x

Crawford IA, Joy KH, Anand M. (2014). Lunar exploration. In Encyclopedia of the Solar System (3rd edition, ed T Spohn, TV Johnson, D Breuer). Elsevier.

Duan, J.F., Zhang, Y., Cao, J.F. (2019). A summary of orbit determination for Chinese lunar exploration project (in Chinese). Journal of Deep Space Exploration, 6(3):203-209.

Ellis, J. (1983). Deep space navigation with noncoherent tracking data. TDA Progress Report 42, 74, pp.1-12.

Foing, B. H., Racca, G. D., Marini, A., Evrard, E., Stagnaro, L., Almeida, M., & Grande, M. (2006). SMART-1 mission to the Moon: status, first results and goals. Advances in Space Research, 37(1), 6-13.

Goswami, J. N., & Annadurai, M. (2011). Chandrayaan-2 mission. In Lunar and Planetary Science Conference (Vol. 42, p. 2042).

He, G.L., Liu, M., Gao, X., Du, X.M., Zhou, H., & Zhu, H.Q. (2020). A Brief Review of the Chinese Deep Space Stations, IEEE Antennas and Propagation Magazine, to appear.

Harvey, B. (2006). Soviet and Russian lunar exploration. Springer Science & Business Media.

Heiken GH, Vaniman D, French BM (eds). (1991). The Lunar sourcebook: A user's guide to the Moon. Cambridge: Cambridge University Press.

Huang, J., Ji, J., Ye, P., Wang, X., Yan, J., Meng, L., Wang, S., Li, C., Li, Y., Qiao, D. and Zhao, W. (2013). The ginger-shaped asteroid 4179 toutatis: New observations from a successful flyby of Chang'e-2. Scientific reports, 3, p.3411.

Huang, Y., Hu, X., Li, P., Cao, J., Jiang, D., Zheng, W., & Fan, M. (2012). Precise positioning of the chang'e-3 lunar lander using a kinematic statistical method. Chinese Science Bulletin 57, 4545-4551.

Huang, Y., Chang, S., Li, P., Hu, X., Wang, G., Liu, Q., Zheng, W., & Fan, M. (2014). Orbit determination of chang'e-3 and positioning of the lander and the rover. Chinese science bulletin 59, 3858-3867.

Goossens, S., Sabaka, T.J., Wieczorek, M.A., Neumann, G.A., Mazarico, E., Lemoine, F.G., Nicholas, J.B., Smith, D.E. & Zuber, M.T. (2019). High-resolution gravity field models from GRAIL data and implications for models of the density structure of the Moon's crust. Journal of Geophysical Research: Planets.

Klopotek, G., Hobiger, T., Haas, R., Jaron, F., La Porta, L., Nothnagel, A., Zhang, Z., Han, S., Neidhardt, A., & Plötz, C. (2019). Position determination of the chang'e 3 lander with geodetic vlbi. Earth, Planets and Space 71, 23.

Li, C., Liu, J., Ren, X., Mou, L., Zou, Y., Zhang, H., Lü, C., Liu, J., Zuo, W., Su, Y. & Wen, W. (2010). The global image of the Moon obtained by the Chang'E-1: Data processing and lunar cartography. Science China Earth Sciences, 53(8), pp.1091-1102.

Li, C., Wang, C., Wei, Y. & Lin, Y. (2019). China's present and future lunar exploration program. Science, 365(6450), pp.238-239.

Li, C., Liu, D., Liu, B., Ren, X., Liu, J., He, Z., Zuo, W., Zeng, X., Xu, R., Tan, X. & Zhang, X. (2019). Chang'E-4 initial spectroscopic identification of lunar farside mantle-derived materials. Nature, 569(7756), pp.378-382.

Li, C., Liu, J., Ren, X., Zuo, W., Tan, X., Wen, W., Li, H., Mu, L., Su, Y., Zhang, H. & Yan, J. (2015). The Chang'e 3 mission overview. Space Science Reviews, 190(1-4), pp.85-101.

Li, P., Hu, X., Huang, Y., Wang, G., Jiang, D., Zhang, X., Cao, J. & Xin, N. (2012). Orbit determination for Chang'E-2 lunar probe and evaluation of lunar gravity models. Science China Physics, Mechanics and Astronomy, 55(3), pp.514-522.

Liu, J., Ren, X., Yan, W., Li, C., Zhang, H., Jia, Y., Zeng, X., Chen, W., Gao, X., Liu, D. & Tan, X. (2019). Descent trajectory reconstruction and landing site positioning of Chang'E-4 on the lunar farside. Nature communications, 10(1), pp.1-10.

Montenbruck, O., Van Helleputte, T., Kroes, R. & Gill, E., 2005. Reduced dynamic orbit determination using GPS code and carrier measurements. Aerospace Science and Technology, 9(3), pp.261-271.

Nozette, S., Rustan, P., Pleasance, L.P., Kordas, J.F., Lewis, I.T., Park, H.S., Priest, R.E., Horan, D.M., Regeon, P., Lichtenberg, C.L. & Shoemaker, E.M., 1994. The Clementine mission to the Moon: Scientific overview. Science, 266(5192), pp.1835-1839.

579 Ouyang, Z., Li, C., Zou, Y., Zhang, H., Lü, C., Liu, J., Liu, J., Zuo, W., Su, Y., Wen, W. & Bian, W., 2010.
580 Primary scientific results of Chang'E-1 lunar mission. Science China Earth Sciences, 53(11), pp.1565-1581.
581 Ping, J., Su, X., Huang, Q. and Yan, J., 2011. The Chang'E-1 orbiter plays a distinctive role in China's first
582 successful selenodetic lunar mission. Science China Physics, Mechanics and Astronomy, 54(12), pp.2130-2144.
583 Pavlis, D. E. (2001). GEODYN II system documentation. Raytheon ITSS Contractor rep., Greenbelt, MD,
584 2001.
585 Qin, S., Huang, Y., Li, P., Shan, Q., Fan, M., Hu, X. & Wang, G., 2019. Orbit and tracking data evaluation of
586 Chang'E-4 relay satellite. Advances in Space Research, 64(4), pp.836-846.
587 Qin, S., Huang, Y., Li, P., Shan, Q., Fan, M., Hu, X., & Wang, G. (2019). Orbit and tracking data evaluation of
588 Chang'E-4 relay satellite. Advances in Space Research, 64(4), 836-846.
589 Ren, X., Liu, J.J., Li, C.L., et al. (2019). A Global Adjustment Method for Photogrammetric Processing of
590 Chang'E-2 Stereo Images. IEEE Transactions on Geoscience and Remote Sensing. doi:
591 10.1109/TGRS.2019.2908813.
592 Schmidt, G., Daou, D., Pendleton, Y., Morrison, D., & Bailey, B. (2012). The NASA Lunar Science Institute's
593 Three-Year Report. In European Planetary Science Congress 2012.
594 Sjogren, W. L., Trask, D. W., Vegos, C. J., & Wollenhaupt, W. R. (1966). Physical constants as determined
595 from radio tracking of the Ranger lunar probes.
596 Tapley, B.D., Ries, J.C., Davis, G.W., Eanes, R.J., Schutz, B.E., Shum, C.K., Watkins, M.M., Marshall, J.A.,
597 Nerem, R.S., Putney, B.H. & Klosko, S.M. (1994). Precision orbit determination for TOPEX/POSEIDON. Journal
598 of Geophysical Research: Oceans, 99(C12), pp.24383-24404.
599 Uesugi, K., Matsuo, H., Kawaguchi, J. & Hayashi, T. (1991). Japanese first double lunar swingby mission
600 "Hiten". Acta Astronautica, 25(7), pp.347-355.
601 Wilhelms DE. (1993). To a Rocky Moon: A Geologist's History of Lunar Exploration. Tucson: University of
602 Arizona Press.
603 Wu, W., Li, C., Zuo, W., Zhang, H., Liu, J., Wen, W., Su, Y., Ren, X., Yan, J., Yu, D. & Dong, G. (2019).
604 Lunar farside to be explored by Chang'e-4. Nature Geoscience, 12(4), pp.222-223.
605 Yan, J., Goossens, S., Matsumoto, K., Ping, J., Harada, Y., Iwata, T., Namiki, N., Li, F., Tang, G., Cao, J. &
606 Hanada, H. (2012). CEGM02: An improved lunar gravity model using Chang'E-1 orbital tracking data. Planetary
607 and Space Science, 62(1), pp.1-9.
608 Yan, J.G., Ping, J.S., Li, F., et al. (2010). Chang'E-1 precision orbit determination and lunar gravity field
609 solution. Advances in Space Research 46, 50–57.
610 Yan, J., Goossens, S., Matsumoto, K., et al. (2012). CEGM02: An improved lunar gravity field model using
611 Chang'E-1 orbital tracking data, Planetary and Space Science, 62, 1:1-9
612 Yan, J., Ping, J., Li, F., et al. (2010). Chang'E-1 precision orbit determination and lunar gravity field solution,
613 Advances in Space Research, 46, 1:50-57
614 Yan J, Yang X, Ping J, et al. (2018). Simulation of the Chang'E-5 mission contribution in lunar long
615 wavelength gravity field improvement. Astrophysics and Space Science, 363(6): 125.
616 Ye, M., Yan, J., Li, F., et al. 2016, in International Symposium on Lunar and Planetary Science, Wuhan
617 Zheng, Y.C., Tsang, K.T., Chan, K.L., Zou, Y.L., Zhang, F. & Ouyang, Z.Y. (2012). First microwave map of
618 the Moon with Chang'E-1 data: The role of local time in global imaging. Icarus, 219(1), pp.194-210.
619 Zhou, J., Liu, Y., Peng, D., & Zhao, F. (2011). Chang'E-2 satellite asymmetric-descent orbit control
620 technology. Science China Technological Sciences, 54(9), 2247.
621 Zuber, M.T., Smith, D.E., Watkins, M.M., Asmar, S.W., Konopliv, A.S., Lemoine, F.G., Melosh, H.J.,
622 Neumann, G.A., Phillips, R.J., Solomon, S.C. & Wieczorek, M.A. (2013). Gravity field of the Moon from the
623 Gravity Recovery and Interior Laboratory (GRAIL) mission. Science, 339(6120), pp.668-671.